

THE DETECTION AND PROCESSING OF PULSAR SIGNALS
AT DECAMETRIC WAVELENGTHS

Thesis .

Submitted in partial fulfilment of the requirement
for the degree of

DOCTOR OF PHILOSOPHY

by

AVINASH ANANT DESHPANDE

ELECTRICAL ENGINEERING DEPARTMENT


INDIAN INSTITUTE OF TECHNOLOGY , BOMBAY

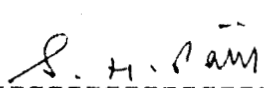
1987

THESIS APPROVAL SHEET

Thesis entitled : THE DETECTION AND PROCESSING OF PULSAR
SIGNALS AT DECA-METRIC WAVELENGTHS by AVINASH ANANT DESHPANDE
is approved for the degree of DOCTOR OF PHILOSOPHY.

Examiners

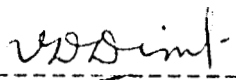




Supervisor(s)



Chairman



9-6-88

CONTENTS

	LIST OF FIGURES	... iv
	LIST OF TABLES	... viii
	NOMENCLATURE	... ix
CHAPTER	1 INTRODUCTION AND HISTORICAL REVIEW	
	1.1 Introduction	... 1
	1.2 Radio Emission from Pulsars	... 2
	1.3 Observational Properties of Pulsars	... 7
	1.4 Pulsar Signal Processing Techniques	... 11
	1.5 Pulsar Observations at Decametric Wavelengths	... 15
CHAPTER	2 THE DECAMETER-WAVE RADIO-TELESCOPE AT GAURIBIDANUR AND THE NEW TRACKING SYSTEM	
	2.1 Introduction	... 25
	2.2 The Decameter-wave Radio-telescope at Gauribidanur	... 26
	2.3 System Capabilities	... 39
	2.4 The Tracking System	... 43
CHAPTER	3 PULSAR OBSERVATIONS WITH THE SINGLE FREQUENCY-CHANNEL RECEIVER	
	3.1 Introduction	... 70
	3.2 Observations of Low Dispersion Measure Pulsars	

	3.3	Flux Calibration	... 92
	3.4	Estimation of the Average Pulse Energy and the Amount of Interstellar Scattering	... 95
	3.5	Fluctuation Spectra	... 96
	3.6	Low Frequency Variability	... 100
CHAPTER	4	OBSERVATIONS OF HIGHLY DISPERSED PULSAR SIGNALS	
	4.1	Introduction	... 104
	4.2	Basic Scheme : Swept-frequency Dcdispersion	... 105
	4.3	The Sweeping Local Oscillator System (SLOS)	... 108
	4.4	New Scheme for Gain Calibration	... 130
	4.5	Procedures for Observations and Data Acquisition	... 140
	4.6	Data Processing and Detection	... 144
	4.7	Conclusion	... 149
CHAPTER	5	RESULTS AND DISCUSSION	
	5.1	Introduction	... 151
	5.2	PSR 0628-28	... 152
	5.3	PSR 0809+74	... 156
	5.4	PSR 0834+06	... 156
	5.5	PSR 0942-13	... 160
	5.6	PSR 0943+10	... 160
	5.7	PSR 0950+08	... 167

5.8	PSR 1133+16	...	167
5.9	PSR 1919+21	...	171
5.10	Scattering in the Interstellar Medium	...	171
5.11	Summary	...	178
CHAPTER 6	CONCLUSIONS	...	180
APPENDIX I	APPARENT PERIODS OF PULSARS	...	186
APPENDIX II	PROPAGATION EFFECTS IN THE INTERSTELLAR MEDIUM	...	189
APPENDIX III	DEFINITIONS	...	198
APPENDIX IV	THE SIGNAL-TO-NOISE RATIO OBTAINABLE WHEN COS AND SIN CORRELATIONS ARE SQUARED, ADDED AND SQUARE ROOTED	...	200
APPENDIX V	OPTIMUM COMBINATION OF TWO INDEPENDENT ESTIMATES	...	207
	REFERENCES	...	210
	ACKNOWLEDGEMENTS		
	SUMMARY		

LIST OF FIGURES

Figure		page
1.1	Number of pulsars observed Vs. the frequency of observation.	... 16
2.1	Schematic of the dipole.	... 27
2.2	The basic array element.	... 28
2.3	The "T" array.	... 29
2.4	(a) Configuration within each EW group.	... 30
	(b) Combination of the groups in the EW array.	... 32
2.5	Configuration in the South array.	... 33
2.6	Block diagram of the analog receiver.	... 36
2.7	Block diagram of the Autocorrelation Receiver [Udayashankar,N.,1986][87].	... 38
2.8	(a) Introduction of new phase shifters ϕ_1, ϕ_2 50
	(b) Introduction of new phase shifters ϕ_3, ϕ_4, ϕ_5 51
2.9	Phase gradients and the required compensation.	... 52
2.10	The phase shifter module.	... 54
2.11	Location of the pre-amplifier.	... 57
2.12	Block diagram of the timing controller.	... 61

	A scheme to obtain 4-bit representations for $\phi_1 \rightarrow \phi_5$... 63
2.14	Generation of all the required control sets from the output of the Beam Counter.	... 65
2.15	The driver/display module : circuit diagram.	... 67
2.16	A point source observation with the tracking system.	... 69
3.1	A flow chart of the data logger operations.	... 73
3.2	Block diagram of the data logging system.	... 75
3.3	Arrangement for the receiver gain calibration.	... 78
3.4	Average profile in the COS and the SIN channels.	... 86
3.5	An average profile obtained by combining the COS and the SIN channel outputs using the new procedure.	... 93
3.6	Fluctuation spectra Vs. longitude for PSR 0834+06 at 34.5 MHz	... 101
4.1	Time to frequency mapping of dispersed pulsar signals.	... 106
4.2	The swept-frequency dedispersion scheme.	... 109
4.3	A plot of pulsar periods Vs. DMs.	... 110
4.4	(a) The required sweep frequency $f_3(t)$. (b) A simplifying approximation for sweep frequency.	... 114
4.5	A basic design for the SLOS.	... 116

4.6	Design of the sweep controller.	... 118
4.7	A design for the controlled oscillator using a DAC and a VCO.	... 120
4.8	The basic divide-and-add scheme for a controlled oscillator.	... 122
4.9	A four stage divide-and-add scheme for the controlled oscillator.	... 124
4.10	Design of the programmable divider.	... 127
4.11	Design of the frequency adder module.	... 129
4.12	The distribution of errors in the final output frequency of the SLOS.	... 131
4.13	The basic receiver set-up used for observations of highly dispersed pulsar signals.	... 141
4.14	Average profile of PSR 1919+21 using the swept-frequency dedispersion scheme,	... 150
5.1	(a) Average profile of PSR 0628-28 using the swept-frequency dedispersion scheme.	... 153
	(b) Average profile of PSN 0628-28 using the single frequency channel scheme.	... 154
5.2	Energy spectrum of PSR 0628-28.	... 155
5.3	Average profile of PSR 0809+74 using the single frequency channel scheme.	... 157
5.4	Energy spectrum of PSR 0809+74.	... 158
5.5	(a) Average profile of PSR 0834+06 using the single frequency channel scheme.	... 159
	(b) Average profile of PSR 0834+06 using	

	the swept-frequency dedispersion scheme.	... 161
5.6	Energy spectrum of PSR 0834+06.	... 162
5.7	Average profile of PSR 0942-13 using the single frequency channel scheme.	... 163
5.8	Average profile of PSR 0943+10 using the single frequency channel scheme.	... 165
5.9	Average profile of PSR 0943+10 using the swept-frequency dedispersion scheme.	... 166
5.10	Average profile of PSR 0950+08 using the single frequency channel scheme.	... 168
5.11	Energy spectrum of PSR 0950+08.	... 169
5.12	Average profile of PSR 1133+16 using the single frequency channel scheme.	... 170
5.13	Energy spectrum of PSR 1133+16.	... 172
5.14	Average profile of PSR 1919+21 using the swept-frequency dedispersion scheme.	... 173
5.15	Energy spectrum of PSR 1919+21.	... 174

LIST OF TABLES

Table		page
2.1	OPERATING MODES OF THE GAURIBIDANUR TELESCOPE WITH THE CORRESPONDING BEAM WIDTHS AND EFFECTIVE COLLECTING AREA	... 34
3.1	RELEVANT PARAMETERS OF 20 PULSARS	... 79
3.2	LIST OF CALIBRATION SOURCES AND THEIR ASSUMED FLUXES	... 94
3.3	ESTIMATES FOR THE AVERAGE PULSE ENERGY AND THE AMOUNT OF SCATTERING	... 97

NOMENCLATURE

ALPHABETS

a	Characteristic scale size of electron density fluctuations.
a1	= $\langle A1 \rangle$
a2	= $\langle A2 \rangle$
a(t)	Calibrated profile.
Ampl1,Ampl2	Best fit amplitudes.
A3,A4	Random variables.
Ae	Effective aperture size.
Ao	New estimate using A1 and A2 .
Ao1,Ao2	Two independent estimates of a quantity.
A(I)	Bin contribution in Ith bin.
Ao(t)	COS channel output when $\Delta \theta = 0$.
Ac(t)	Average profile in COS channel.
As(t)	Average profile in SIN channel.
Ave(I)	Average profile over 2-period stretch.
b	$= (a1^2 + a2^2)^{1/2}$
b1-->b8	8-bit binary number corresponding to ϕ_1
B	Predetection bandwidth.
B _o	Magnetic flux density.
B5-->B0	6-bit output of the beam counter.
BFT	"Beam flipping time" in tracking .

B_{opt}	Optimum bandwidth,
$B(t)$	Sample value at time t .
	The velocity of light.
	Mean number of samples averaged.
C_{ji}	1-bit control signal for phase shifter.
$C(I)$	Effective number of samples averaged in I th bin.
	Distance to a pulsar.
d'	Constant to account for average gain of the EW beam over 30' arc.
d_1	Distance between two basic array elements in E-W direction.
$d(t)$	The receiver bandpass converted into time function by the dispersion law.
$(df/dt)_d$	Drift rate due to $AP \neq 0$.
$(df/dt)_{sw}$	Sweep rate of the SLOS.
D_0	Calibrator deflection corrected for collimation error.
D_c	Calibrator deflection in COS channel.
DM	Dispersion Measure.
D_n	Deflection due to calibration noise.
D_s	Calibrator deflection in SIN channel.
e	Charge of an electron.
f, f_1, f_2	Radio frequencies in Hz.
f_0	Centre frequency of observation.
f_{clk}	Sampling clock frequency.
f_s, f_e	Start and end frequency of the sweep.

f_{in}, f_x	First and second input frequency.
f_{LF}	Frequency of low frequency signal.
f_{RF}	Frequency of RE' signal.
$f(t)$	Staircase function as an approximation to $f_{\lambda}(t)$.
$f_{out}(t)$	Output frequency of the sweeping LO system.
$f_{\lambda}(t)$	Required frequency.
$F(t)$	Best fit profile.
g_c	Gain factor due to collimation error.
\bar{g}	Average gain.
$g(n)$	Actual gain function in the frequency domain.*
$g(t)$	Best fit function to an observed profile.
$g_o(n)$	Crude estimate of $g(n)$.
$g_l(n)$	Modified gain function.
$g'(n)$	Effective gain function in the frequency domain.
G_a	Gain function of the telescope upto mixer stage.
G_b	Gain of the baseband filter.
G_c	Gain of the correlation beam.
G_e, G_w	Phase gradients for East and West arrays.
$ G _{max}$	Maximum value of the phase gradient, Running index.
$i(t)$	Function representing intrinsic pulse profile. Integral number of Lines in the fraction of the Np-period stretch.
\bar{I}_B	Average intensity of the background radiation.
ICH	Channel index.
\bar{I}'_B	Background noise intensity off the source.

$I(t)$	Intensity due to a pulsar signal at the output of a receiver.
$\bar{I}(n)$	Average intensity pattern in frequency domain.
$I_B(f_{RF}, t)$	spectral density of background radiation at the antenna input.
$I_{off}(n)$	Measured intensities off the source.
$\bar{I}_p(\phi_s(n))$	Average intensity of a pulsar signal at longitude $\phi_s(n)$.
$I_p(f_{RF}, t)$	Spectral density of a pulsar signal at the input of the Antenna.
k	Boltzman's constant.
k_0, k'	Constants.
K	System gain normalization factor.
K_0	A constant.
L	Lower sideband intensity.
L_0	Integer number.
L_c	Length of a phase cable.
L_{EW}	Length of the EW array.
m	Mass of an electron.
m'	Receiver dependent constant.
\bar{m}	Modulation index.
n, n'	Bin index.
n_0	Number of observations.
n_1, n_2	Zero mean random noise processes.
n_b	Beam position.
n_e	Electron density.

\hat{n}	Step number corresponding to the SLOS frequency.
\hat{n}_s	Step number corresponding to f_s .
n_{samp}	Number of independent samples averaged after post-detection integration.
$n_d(t)$	Number of bins by which pattern drifts in time t .
N	Divisor value.
NB	Number of output bins.
NCH	Number of channels.
N_d	Number of drift cycles.
N_j	Divisor value for j th stage.
N_p	Number of periods over which data is averaged.
N_{rec}	Number of records used for averaging.
N_S	Integral number of N_p -period stretches.
P	Apparent period of a pulsar,
P'	Sweep reset interval.
\dot{P}	First derivative of pulsar period.
\ddot{P}	Second derivative of pulsar period.
P_0, P_1	Pulsar period as would be observed at the Barycentre of the Solar System (BSS) at epochs t_0, t_1 .
P_{noise}	Average power due to background noise .
Q	Level of detection.
r_0	The classical radius of electron.
r_ρ	Spatial scale of a diffraction pattern at the Earth.
\vec{r}	Unit vector along the line of sight to a pulsar.

$r(t)$	Impulse response of the post-detection filter.
$R("x")$	Beam pattern in "x" mode.
RA	Right Ascension.
Rcal	Calibration factor (Jansky/count of deflection).
RM	Rotation measure.
$R_j(\theta_m)$	Ratio of the secondary response to the main response of the EW array.
ReE 3	Real part.
$s(t)$	Impulse response due to interstellar scattering.
\bar{S}	Average of S_i .
S	Source strength in Jansky.
$(S/N)_{A_i}$	Signal-to-noise ratio for A_i .
SINC(Y)	= $\text{SIN}(Y)/Y$
S_i	Pulse energy estimate in i th observation.
SLOS	Sweeping Local Oscillator System.
t	Time co-ordinate.
t_0, t_1	Epochs.
t_1, t_2	Pulse arrival times.
t'_i	= $t - iP$ (for $i=0,1,\dots$), such that $0 \leq t'_i < P$
t''	= t' / DM
t_{off}	Duration of off-source observation.
t_{on}	Duration of on-source observation.
t_s, t_e	Start and end time for tracking.
T_s	Sampling interval.
T_{sys}	System noise temperature.
U	Upper sideband intensity.

V_d	Projected velocity of an observatory in the direction of a pulsar.
\vec{V}_E	A velocity vector representing the velocity of the geocentre with respect to the BSS.
V_g	Group velocity.
\vec{V}_{obs}	Velocity of an observatory with respect to the geocentre.
V_s	Velocity of the earth-pulsar line across the scattering screen.
V_x, V_y, V_z	Components of \vec{V}_E .
$V(t)$	Complex envelope associated with $X(t)$. Undispersed pulse width.
$W1, W2$	Weightages. A constant with value close to unity.
$X(t)$	Varying voltage due to a pulsar signal.
γ	$(\text{Amp1}^2 + \text{Amp2}^2)^{1/2} / g_c$ Zenith angle.

Greek Symbols

β	Velocity factor of the cable.
Υ	Increase in time resolution.
δ	Declination.
δf	Spectral resolution or binwidth.
$\delta f(t)$	Error in f_{out} .

δt	Additional smearing in time.
$\delta \Psi$	Difference between Faraday rotation angles at the extreme frequencies within a band ΔF .
ΔBFT	Absolute quantization error in representing BFT.
Δf	Bandwidth over which a pulsar profile over one period gets mapped in frequency.
ΔF	$f_2 - f_1$
$\Delta g(n)$	Error in the estimation of $g(n)$.
ΔI	Fraction of the bin.
$\Delta I_{off}(n)$	Error in the estimation of $I_{off}(n)$.
ΔI_p	Uncertainty in estimation of $I_p()$.
Δn_e	Electron density fluctuations.
ΔP	Deviation of reset interval(P') from P .
ΔRA	Absolute quantization error in representing RA.
Δt	Step width in $f(t)$.
Δt	$t_2 - t_1$
Δt_{bin}	Binwidth in time.
Δt_{φ}	Worst case error in t_s, t_e due to ΔRA and ΔBFT .
ΔT_{amp}	Sampling interval.
$\Delta \theta$	Effective collimation error in N-S direction.
$\Delta \Psi$	Faraday rotation angle.
$\Delta \nu$	Decorrelation bandwidth for interstellar scintillation.
$\Delta \phi$	r.m.s. phase deviation due to scattering.
η	Delay decorrelation factor.
θ	Angle between the line of sight and the

	direction of interstellar magnetic field.
θ_0	Apparent angular semidiameter of a source due to scattering.
θ_b	Peak to first null separation of the basic array element beam in EW direction.
θ_m	Angular tilt from the meridian.
θ_{NS}	Peak to first null separation of the S arm beam in NS direction.
θ_s	Scattering angle.
λ	Wavelength.
ρ_a	Normalized analog correlation.
ρ_c	Normalized one-bit correlation.
σ_T	Estimate of the standard deviation of noise in the profiles $A_c(t), A_s(t)$.
σ	Standard deviation due to noise.
σ_1, σ_2	r.m.s. noise in the estimates A_{o1} and A_{o2} .
σ_i	Standard deviation of data in i th record before averaging.
σ_0	r.m.s. noise deviation in the A_0 .
σ_N	Standard deviation of A_4 from its true value b .
σ	Standard deviation of noise in output profile.
τ	Post-detection integration time.
$\bar{\tau}$	Mean uncompensated delay.
τ_{max}	Maximum delay.
τ_{on}	On-line integration time.
τ_d	Decorrelation time for interstellar

scintillations.

τ_s Characteristic width of the impulse response
due to scattering.

ϕ Phase shift.

1 - Phase shifts required for tracking.

$\phi_s(n)$ Longitude of a pulsar signal at frequency
($f_s + n\delta f$) and time $t = 0$.

ω Frequency in radians per second.

Plasma frequency in radians per second.

Suffix

max Maximum value.

min Minimum value.

r.m.s. Root mean squares.

Other Symbols

Frac() Fraction.

Int() Interger part.

\sum Summation.

|| Magnitude.

*

Dot product.

$\langle \rangle$ Ensemble mean.